

Observation of Quantum Beats in the Resonance Fluorescence of Free Excitons

V. Langer, H. Stolz, and W. von der Osten

Universität Gesamthochschule Paderborn, D-4790 Paderborn, Federal Republic of Germany

(Received 26 June 1989)

The occurrence of quantum beats for an extended exciton state in a solid is demonstrated for the first time. They are observed as oscillations in the 2TO(L) phonon-assisted fluorescence resonance fluorescence decay of the indirect free exciton states in AgBr split in magnetic fields up to 1 T after excitation by picosecond laser pulses. The results are in agreement with calculations by a density-matrix formalism. From the beating frequencies the splitting of the exciton states can be obtained with high accuracy. Quantum dephasing times of several hundred picoseconds are determined, comparable to the energy relaxation time.

PACS numbers: 42.50.Md, 71.35.+z, 78.47.+p

To completely describe the relaxation of elementary electronic excitations like excitons or electron-hole pairs in semiconductors and ionic crystals, the coherence properties of the quasiparticles are of importance. While the relaxation processes are usually discussed in terms of occupation probabilities that are related to the diagonal elements of the density matrix ρ of the system in question, coherence is directly connected with the off-diagonal elements, generally giving rise to two types of coherence phenomena. One is *optical coherence* between the ground and excited states whereby the electronic excitations are coupled to the phase of an electromagnetic wave.¹ The other is *quantum coherence* between excited electronic states that are closely adjacent in energy. The conceptionally clearest way to demonstrate quantum coherence is by means of *quantum beats* in the time-resolved fluorescence originating from a coherent superposition of the participating excited states.² The preparation of this coherence may be accomplished by simultaneous excitation of the states by a light pulse with a duration short compared to the reciprocal of the splitting frequency. The temporal evolution of the coherence shows up as oscillation in the decay of the polarized fluorescence intensity. While the beating frequency is determined by the energy splitting of the excited states, the damping of the oscillation gives direct information on the quantum dephasing time independent of any inhomogeneous broadening of the states.

Investigations of coherence phenomena involving extended electronic states in solids were recently reported in which various pump and probe techniques, like transient four-wave mixing³⁻⁵ or induced absorption,⁶ were employed to probe optical coherence on time scales down to several femtoseconds. In contrast, quantum coherence of these states, which might be rather different, up to now was investigated only indirectly by studying the polarization properties of the emission processes, either stationary⁷ or time resolved.^{8,9} The direct observation of quantum coherence through quantum beats, however, so far is restricted to atoms and molecules in gases and liquids where this method is established as a powerful spectroscopic tool to explore in detail both electronic and vibrational states (see Refs. 2, 10, and 11).

In this paper, we report the first observation of quantum beats for an extended (free) exciton state in a crystalline solid. As a model system we investigated the lowest $\Gamma_6^+ \otimes L_{4,5}$ exciton in AgBr that was already thoroughly studied in the past (see, e.g., Ref. 9). Because of its indirect character (minimum of the valence band at the L point of the Brillouin zone), the exciton absorption and emission processes are each associated with a momentum-conserving phonon. As schematically illustrated by the inset in Fig. 1 the resonance fluores-

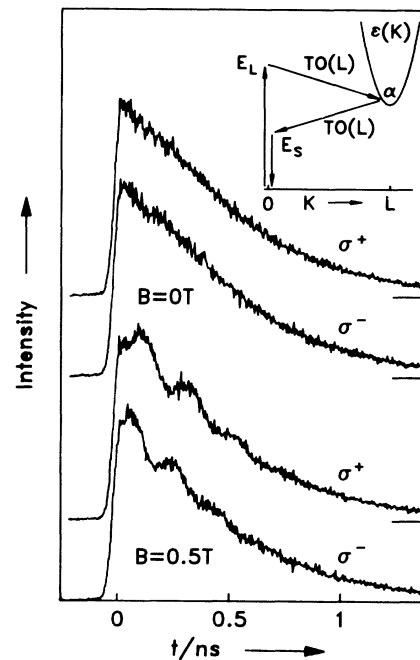


FIG. 1. Time dependence of polarized 2TO(L) intensity for an oriented AgBr crystal at 2 K. Excitation with an 8-ps laser pulse at $E_L = 2.6931$ eV polarized along $[1\bar{1}0]$. Direction of observation is along $[001]$ with left (σ^+) and right (σ^-) circular polarization. Inset: The 2TO(L) phonon-assisted scattering process corresponding to the RF of the indirect exciton in AgBr at the L point [2TO(L)]. $\epsilon(\mathbf{K})$: exciton dispersion; E_S : scattered photon energy; α : intermediate exciton states monitored by the 2TO(L) process.

cence (RF), which may be equally regarded as resonant Raman scattering,⁹ therefore consists of various sharp two-phonon lines. By monitoring the polarized intensity of the dominant 2TO(*L*) scattering process after short-pulse excitation, it is possible to directly probe the relaxation behavior of the exciton states. If the degenerate exciton states are split in a magnetic field,¹² the coherent excitation of the sublevels leads to quantum beats in the scattered intensity.

To detect the modulation in the decay of the RF the time response of the spectroscopic apparatus has to be sufficiently fast. On the other hand, high spectral resolution is required because the fluorescence spectrum consists of a large number of lines originating from the emission of free excitons with different **K** states and various types of bound-exciton transitions. A prerequisite for detecting quantum beats therefore is a spectral and temporal resolution which is limited by the energy-time uncertainty. To achieve this, in our experimental setup the RF was spectrally analyzed by means of a high-resolution double monochromator (focal length of 1 m) with subtractive dispersion to compensate the light transit-time spread of a single grating. As tested by a synchroscan streak camera as detector, transform-limited performance could be obtained down to about 8 ps. In the measurements reported here, we employed a microchannel-plate photomultiplier as detector because of its better sensitivity. The overall system response to the laser pulse in this case was better than 40 ps FWHM. Excitation was accomplished with pulses of about 8-ps duration and 0.3-meV spectral width from a dye laser (Stilben 3, average power 10 mW), which was pumped synchronously by the 365-nm line of a mode-locked Ar⁺ laser (pulse width 25 ps, 120 mW power). The oriented sample at 2 K was placed in a superconducting-magnet cryostat (*B* < 4.5 T) with the magnetic field along the [001] (**z**) direction. The incident laser beam was parallel to [110] (**y**) with polarization along [110] (**x**), while the scattered light was observed in a Faraday configuration under 90°.

Representative decay curves of the 2TO(*L*) intensity detected with left (σ^+) and right (σ^-) circular polarization are displayed in Fig. 1 for an excitation photon energy E_L slightly (0.4 meV) above the exciton absorption threshold at $E_a^i = 2.6927$ eV. Following the fast rise determined by the width of the laser pulse, for zero magnetic field (upper curves) in both polarizations the signal decays by the same single exponential (apart from a minor deviation due to the fluorescence background of our dye laser). In contrast, for *B* = 0.5 T a superimposed modulation of the scattered intensity is clearly visible, which unambiguously proves the occurrence of the expected quantum beats. For the case displayed, the intensity oscillates with a period of about 200 ps being phase shifted by 180° between σ^+ and σ^- polarization. Similar results were found for other directions of polarization and for magnetic fields up to *B* = 1 T.

As known from stationary resonant Raman scattering in magnetic fields,¹² at zero field the fourfold-degenerate exciton states $\psi_i = |\sigma_z, s_z\rangle$ consist of a pair of degenerate singlet-triplet states $\psi_1 = |\frac{1}{2}, \frac{1}{2}\rangle$, $\psi_4 = |-\frac{1}{2}, -\frac{1}{2}\rangle$ and a pair of optically forbidden pure triplet states $\psi_2 = |\frac{1}{2}, -\frac{1}{2}\rangle$, $\psi_3 = |-\frac{1}{2}, \frac{1}{2}\rangle$ split by the exchange interaction (σ_z, s_z denote effective hole and electron spins). The energy shift and mixing of these states in a magnetic field **B** is determined by the effective Hamiltonian:¹²

$$H_{ex} = 2\Delta(\sigma_z s_z - \frac{1}{4}) + g_c \mu_B \mathbf{S} \cdot \mathbf{B} - g_v^{\parallel} \mu_B \sigma_z B_z + \frac{1}{2R^* \mu^{*2}} \mu_B^2 \mathbf{B}^2. \quad (1)$$

The parameters denote the following quantities: Δ is the exchange interaction, g_c, g_v^{\parallel} are the *g* factors of electron and hole states, μ^* is the reduced effective mass of the exciton in units of the free-electron mass, R^* is the excitonic Rydberg energy, B_z is the component of the magnetic field in the [111] direction, and μ_B is the Bohr magneton. As shown by Eq. (1), the quantization axis is always determined by the *L*-point symmetry of the exciton states. Therefore, the chosen orientation of the crystal axis and the magnetic field results in the most simple splitting pattern being the same for all *L* points.

To describe the dynamical behavior and the coherence properties of the exciton system, the density-matrix formalism¹³ has to be applied. Since intervalley mixing of free exciton states is forbidden,¹⁴ the treatment may be restricted to the exciton subspace at one *L* point, the final results being obtained by summing over the four inequivalent *L* points. The time evolution of the density matrix ρ_{ij} made up from the exciton states ψ_i ($i, j = 1, \dots, 4$) is given by the Liouville equation:¹⁵

$$\frac{\partial \rho}{\partial t} = -\frac{i}{\hbar} \mathcal{L} \cdot \rho - \mathcal{R} \cdot \rho + G. \quad (2)$$

Here $\mathcal{L} = [H_{ex},]$ is the Liouville operator of the Hamiltonian [Eq. (1)] and \mathcal{R} is the relaxation operator describing the various decay processes of the density-matrix elements. The generation matrix *G* contains the interaction of the exciton system with the exciting laser light. In the case of broadband illumination,² which applies to our experimental situation (spectral width of exciting laser pulses larger than transform limited), the interaction of the excitons with light via the indirect transition may be approximated by the transition dipole moments of the exciton states,

$$\mathbf{M}_i = \langle \psi_i | \mathbf{D} | 0 \rangle, \quad (3)$$

where $|0\rangle$ is the crystal ground state and **D** is the dipole operator. The form of \mathbf{M}_i is determined by the symmetry of the Bloch states and can be worked out by standard group-theoretical methods.⁹ Using definition (3), *G* is given by^{2,7}

$$G_{ij} \propto \sum_{\alpha, \beta} (\mathbf{M}_i \cdot \mathbf{e}_\alpha) (\mathbf{M}_j \cdot \mathbf{e}_\beta)^* I_{\alpha\beta}^0 \quad (4a)$$

with $\mathbf{e}_{\alpha,\beta}$ the polarization vectors and $I_{\alpha\beta}^0$ the polarization density matrix ($\alpha,\beta=x,z$) of the exciting laser light.¹³ In the same approximation, the polarization density matrix of the RF intensity can be written

$$I_{\alpha\beta}^{\text{RF}} \propto \sum_{i,j} (\mathbf{M}_i \cdot \mathbf{e}_\alpha)^* (\mathbf{M}_j \cdot \mathbf{e}_\beta) \rho_{ij}. \quad (4b)$$

The solution of Eq. (2) can be simplified considerably by realizing that at low fields ($B < 1$ T) magnetic-field-induced mixing of the exciton states is small and contributions from the triplet states ψ_2 and ψ_3 can be neglected (transition strength $< 10\%$ of that of singlet-triplet states¹²). In this low-field limit the density matrix transforms under the symmetry operations of the L point (D_{3d}) according to the product representation $L_3^- \otimes L_3^- = L_1^+ + L_2^+ + L_3^+$. Thus ρ can be decomposed into irreducible components each of which decays with its own characteristic time constant. These relaxation times completely determine the relaxation operator \mathcal{R} containing phenomenologically the exciton relaxation processes. The components of ρ are the total exciton population $\rho^{(1)} = \rho_{11} + \rho_{44}$ (decay by energy relaxation with rate $1/\tau_0$), the difference in exciton population $\rho^{(2)} = \rho_{11} - \rho_{44}$ (decay with rate $1/\tau_2$), and $\rho^{(3)} = (\rho_{14} + \rho_{41}, \rho_{14} - \rho_{41})$, which represent the real and imaginary parts of the off-diagonal elements decaying with quantum dephasing rate $1/\tau_{\text{coh}}$, respectively.

From Eqs. (2)–(4) the time dependence of the RF intensity of the 2TO(L) process after δ -pulse excitation and for the conditions of light polarizations in Fig. 1 is finally obtained as

$$I(\sigma^\pm, t) \propto e^{-t/\tau_0} \mp \frac{1}{3} \left(\frac{2}{3}\right)^{1/2} e^{-t/\tau_{\text{coh}}} \sin(2\pi\nu_{41}t). \quad (5)$$

In deriving this expression, the transition moments parallel and perpendicular to the [111] direction⁹ were assumed to be equal, as justified by the experimental results. Furthermore, in the exciton density matrix only states with the same wave vector need to be considered and give rise to quantum interference effects. Because of the finite spectral bandwidth of excitation RF comes from different noninterfering \mathbf{K} states resulting in an additional background on which the quantum beats are superimposed.

The beating frequency $\nu_{41} = \Delta E_{41}/h$ between states 1 and 4 is obtained by diagonalization of H_{ex} [Eq. (1)] in the low-field limit as

$$\nu_{41} = \frac{1}{\sqrt{3}h} (g_{\parallel} - g_{\perp}) \mu_B B + \frac{(g_{\perp} \mu_B B)^3}{3\sqrt{3}\Delta^2 h}. \quad (6)$$

In complete agreement with the experimental observations (Fig. 1), Eqs. (5) and (6) imply that, for both polarizations, at zero field ($\nu_{41} = 0$) the RF signal decays with a single time constant which is determined by the energy relaxation time τ_0 , while for $\mathbf{B} \neq 0$ a superimposed oscillatory structure develops which is phase shifted for σ^+ and σ^- by 180° and decays with the dephasing time τ_{coh} . This oscillation shows up more clearly if the

difference between the right and left circular polarizations is plotted, since in this case the nonoscillating background vanishes according to Eq. (5). This is demonstrated in Fig. 2 for two different field strengths. As illustrated by the heavy line for $B = 0.5$ T, which represents a fit of Eq. (5) to the experimental data, the measurements are well described by the theory developed. From the fit the beating frequency ν_{41} and the quantum dephasing time τ_{coh} are derived to be $\nu_{41} = 5.12$ GHz and $\tau_{\text{coh}} = 400$ ps, whereas the energy relaxation time amounts to $\tau_0 = 450$ ps. For $B = 1$ T the corresponding quantities are estimated as $\nu_{41} \approx 11.6$ GHz and $\tau_{\text{coh}} \approx 300$ ps although the signal-to-noise ratio is worse, which is mainly caused by an increased contribution of noninterfering exciton states with different \mathbf{K} vectors in the RF. The dependence of the beating frequency on magnetic field strength obtained from the measurements is shown in Fig. 3 together with a fit of Eq. (6) to the experimental points. The fitting parameters given in the figure are in good agreement with the high-field values.¹² This fully confirms that the oscillations observed are indeed due to quantum beats of the indirect exciton states.

As known from previous studies of time-resolved RF,⁹ in the energy range slightly above the exciton band bottom trapping at impurities and exciton scattering with long-wavelength LA phonons contribute to the energy relaxation time τ_0 . From the parameters given there, at $\epsilon(\mathbf{K}) = 0.4$ meV a phonon scattering time of 6.6 ns is calculated, implying that the measured relaxation time τ_0 is determined by impurity capture.

Besides by energy relaxation, quantum dephasing is

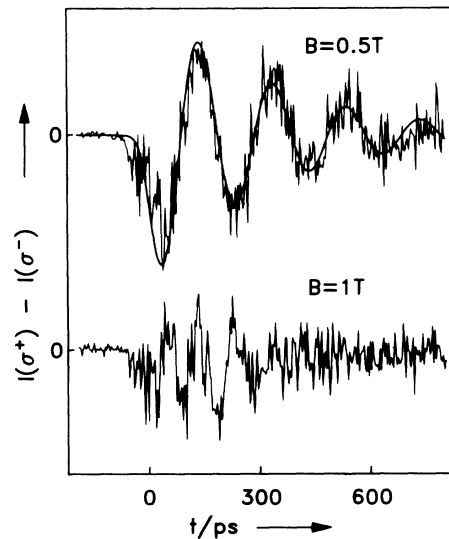


FIG. 2. Difference between right and left circularly polarized RF for two different magnetic field strengths. Experimental data are shown together with a fit for $B = 0.5$ T according to Eq. (5) (heavy line) after convolution with the system response to the laser pulse.

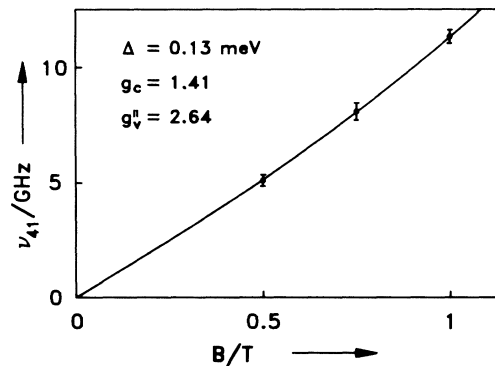


FIG. 3. Frequency difference between sublevels as a function of magnetic field. Points: experimental data from oscillation frequencies; solid line: fit according to Eq. (6) using the parameters as indicated.

affected by elastic scattering, resulting in a relation $1/\tau_{\text{coh}} = 1/\tau_0 + w$, where w takes into account all "pure" dephasing processes linked to the degrees of freedom of the states. For excitons these are the center-of-mass and relative motions of electron and hole characterized by the wave vector \mathbf{K} and the envelope wave function, respectively. At low exciton density in our experiments, exciton-exciton scattering which dephases both types of motion can be excluded. Changes in \mathbf{K} therefore are caused by elastic scattering at defects or by phonon scattering which in first order is always connected with loss in exciton energy and contributes to τ_0 . Dephasing of the relative motion is only possible by elastic processes. Obviously, our results show that the quantum coherence time for exciton energies near the band bottom is almost completely determined by energy relaxation processes. Purely elastic quantum-dephasing scattering is less important indicating a low impurity content of our crystal and high sample quality.

Our results for the quantum dephasing times in AgBr are quite different from the exciton optical coherence times in CuCl (Ref. 3) and GaAs,⁴ which are found by transient four-wave-mixing measurements to be of the order of a few ps. This presumably is related to the inhomogeneous linewidth which is inevitably present for an exciton system due to the dispersion in \mathbf{K} space. While the quantum beat signal is not damped by inhomogeneous broadening nonlinear four-wave mixing is strongly

influenced. Finally, we note that the homogeneous linewidth of the $2\text{TO}(L)$ scattering line is given by the width of the momentum-conserving phonons (0.12 meV as obtained from high-resolution Raman scattering spectra), being much larger than the linewidth of the exciton state itself ($\hbar/\tau_{\text{coh}} \approx 10 \mu\text{eV}$).

Extension of the measurements to higher fields and various exciton kinetic energies, especially in systematically doped samples, is at present in progress.

The authors gratefully acknowledge the support of the project by the Deutsche Forschungsgemeinschaft.

¹L. Allen and J. H. Eberly, *Optical Resonances and Two-Level Atoms* (Wiley, New York, 1975).

²S. Haroche, in *High Resolution Laser Spectroscopy*, edited by K. Shimoda (Springer-Verlag, Heidelberg, 1976).

³Y. Masumoto, S. Shionoya, and T. Takagahara, *Phys. Rev. Lett.* **51**, 923 (1983).

⁴L. Schultheis, J. Kuhl, A. Honold, and C. W. Tu, *Phys. Rev. Lett.* **57**, 1797 (1986).

⁵P. C. Becker, H. L. Fragnito, C. H. Cruz, R. L. Fork, J. E. Cunningham, J. E. Henry, and C. V. Shank, *Phys. Rev. Lett.* **61**, 1647 (1988).

⁶B. Fluegel, N. Peyghambarian, G. Olbright, M. Lindberg, S. W. Koch, M. Joffre, D. Hulin, A. Migus, and A. Antonetti, *Phys. Rev. Lett.* **59**, 2588 (1987).

⁷G. E. Pikus and E. L. Ivchenko, in *Excitons*, edited by E. I. Rashba and M. D. Sturge (North-Holland, Amsterdam, 1982).

⁸R. J. Seymour and R. R. Alfano, *Appl. Phys. Lett.* **37**, 231 (1980).

⁹H. Stolz and W. von der Osten, *Cryst. Lattice Defects Amorphous Mater.* **12**, 293 (1985).

¹⁰M. J. Rosker, F. W. Wise, and C. L. Tang, *Phys. Rev. Lett.* **57**, 312 (1986).

¹¹R. Leonhardt, W. Holzappel, W. Zinth, and W. Kaiser, *Rev. Phys. Appl.* **22**, 1735 (1987).

¹²H. Stolz, W. Wassmuth, W. von der Osten, and Ch. Uihlein, *J. Phys. C* **16**, 955 (1983).

¹³K. Blum, *Density Matrix Theory and Applications* (Plenum, New York, 1981).

¹⁴K. L. Shaklee and R. E. Nahory, *Phys. Rev. Lett.* **24**, 942 (1970).

¹⁵K. E. Jones and A. H. Zewail, in *Advances in Laser Chemistry*, edited by A. H. Zewail, Springer Series in Chemical Physics Vol. 3. (Springer-Verlag, Berlin, 1978), p. 196.